Journal of Applied Polymer Science

Thermo-Reversible Healing in a Crosslinked Polymer Network Containing Covalent and Thermo-Reversible Bonds

Sarah P. Khor, Russell J. Varley, Shirley Z. Shen, Qiang Yuan
CSIRO Materials Science and Engineering, Clayton South, 3169 Victoria, Australia
Correspondence to: R. J. Varley (E-mail: russell.varley@csiro.au)

ABSTRACT: The self-healing behavior of a modified ureido-amide based thermoplastic hybrid elastomer was investigated by increasing the concentration of non-reversible (covalent) bonds compared to reversible (hydrogen) bonds. A crosslinked polymer network was synthesized using varying amounts of diglycidylether of bisphenol A and reacting with the ureido-amide thermoplastic. Increasing epoxy content produced a more rigid and thermally stable hybrid network, which in turn decreased overall thermo-reversible or healing behavior. Fracture toughness recoveries varied from 25% for the system containing the greatest number of covalent bonds to well over 200% for systems containing higher thermoplastic content. Substantial levels of healing, about 62% recovery, were still achieved despite the crosslinked network having a T_g above room temperature, 31°C as measured by differential scanning calorimetry (DSC). Dynamic mechanical thermal analysis was used to monitor thermo-reversible behavior of the elastic moduli and thus probe molecular mobility within the glassy state. The extent and rate of recovery of the elastic modulus was dominated by the extent of thermal activation above the glass transition temperature. Fourier transform infrared spectroscopic and DSC studies confirmed that reacting the thermoplastic with an epoxy resin produced a covalently bonded crosslinked network and the epoxide groups were completely consumed. © 2012 Wiley Periodicals, Inc. J. Appl. Polym. Sci. 128: 3743–3750, 2013

KEYWORDS: crosslinking; mechanical properties; structure–property relations; thermosets; thermoplastics

Received 2 July 2012; accepted 11 September 2012; published online 10 October 2012
DOI: 10.1002/app.38578

INTRODUCTION

Supramolecular polymers containing highly directional but reversible chemico-physical linkages[1] have recently opened a new avenue of research into self-healing polymers.[2,3] The elastomer synthesized in the work by Cordier et al.[2] utilized ureido-amide functional groups in the polymer backbone to elegantly illustrate the ability of hydrogen bonding to produce self-healing behavior after polymer fracture. The low cost nature of the synthesis from readily available materials such as fatty acids, a diamine, and urea in particular provides impetus to the development of new industrial products and commercial applications. Of interest in this work is the use of non-covalent hydrogen bonding to facilitate healing over a number of damage events, which is directly attributable to the thermo-reversible nature of the supramolecular polymer rather than any multi-component approach. This strategy overcomes the restraints of once off repair systems inherent to the more widely studied encapsulation[4] and hollow rod methods.[5] Other thermo-reversible self-healing strategies have been explored, ranging from the application of the reversible Diels–Alder reaction between furan and maleimide,[6] the incorporation of thermoplastic additives into an epoxy resin matrix,[7,8] and ionomers[9] to name few. These strategies, however, tend to require moderately high temperatures to activate healing (>100°C) compared with these supramolecular elastomers which can display self-healing behavior at ambient conditions. Fundamentally, the effectiveness of the self-repair mechanism relies upon the diffusion of molecular chains, so the low glass transition temperature of the elastomer, would indeed be expected to promote reformation of hydrogen bonding at lower temperatures.

The applicability of supramolecular polymers for self-healing systems is therefore self-evident, but their low elastic modulus and strength limits applications to non-structural materials. While self-healing functionality using supramolecular polymers has been used in rubbers[10–12] and thermoplastics,[13,14] to date, there are only a few studies which report on the self-healing behavior of polymer networks containing both covalent non-reversible and thermoreversible bonds in supramolecular systems. Wietor and coworkers[15–17] replaced non-reversible crosslinks with low concentrations of thermoreversible species utilizing hydrogen bonding, and found that the coating produced superior creep and stress relaxation at temperatures below the T_g.

Applied Polymer SCIENCE

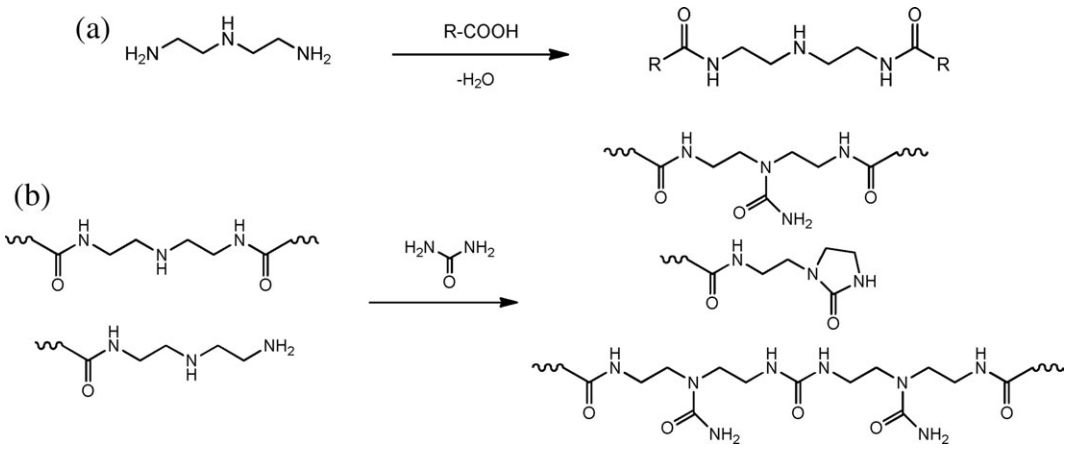

Figure 1. (a) Condensation reaction of diethylene tramine and Empol fatty acid to produce oliogoamidoamine. (b) Addition of urea to form supramolecular elastomers capable of forming multiple hydrogen bonds.

This was attributed to the association and dissociation kinetics of the dimerization of the ureidopyrimidinone crosslink unit, which allows for fast stress relaxation at elevated temperature, but also slow stress relaxation at lower temperature. Montarnal and coworkers (2009)[3,18,19] also sought to explore new material properties by combining supramolecular heterocyclic urea with epoxy resin chemistry to produce hybrid covalent and noncovalent polymer networks. By controlling stoichiometries and side reactions they were able to control whether a material behaved as an elastomer or a thermoset.

Previous studies on supramolecular ureido-amide thermoplastic elastomer as self-healing polymers have focused on the ability of the reversible hydrogen bonding to effect healing. To this end, these elastomers have been shown to be very effective for recovering their adhesion and elongation to failure.[2] However, there are few reports which explore hybrid networks containing both noncovalent, (ionic or hydrogen bonds for example), and covalent crosslinking to evaluate their healing efficiency. This article therefore, will explicitly incorporate increasing levels of covalent crosslinking into a supramolecular ureido-amide thermoplastic elastomer[2] to produce networks with both covalent and hydrogen bonding crosslinks. Covalent crosslinking will come from the use of a diglycidyl ether of bisphenol A (DGEBA), a common di-functional epoxy resin while the ureido-amide thermoplastic elastomer will create the environment for hydrogen bonding. The impact on healing or thermoreversible behavior will be evaluated using dynamic mechanical analysis (DMTA) and single end notched beam (SENB) fracture toughness measurements while the scanning electron microscopy (SEM) will explore the recovery mechanism of the fracture properties. In addition to this, the final polymer network was evaluated using Fourier transform infrared spectroscopy (FTIR) and differential scanning calorimetry (DSC) in order to better understand the reaction between the epoxy resin and the supramolecular ureido-amide thermoplastic.

MATERIALS AND EXPERIMENTAL

Preparation of Epoxy-Ureido Amide Blend

Synthesis of the ureido-amide thermoplastic elastomer was conducted using Empol 1008 (Cognis, OH, USA) a fully hydrogenated dimer fatty acid, DEH20 (Dow, Australia) diethylene triamine (DETA Sigma, Australia), and urea (Sigma, Australia) in accordance to methods outlined by Cordier and coworkers.[2,3] Figure 1 outlines a generalized reaction mechanism of the synthesis of the supramolecular polymer because the Empol 1008 is a dimer fatty acid which is a complex blend of varying carbon long chain species. The first step consists of the (a) condensation between the Empol fatty acid and DETA to form oliogoamido amine products, followed by (b) the addition of urea to produce supramolecular polymers capable of multiple hydrogen bonding. Condensation to amido-amine oligomers was conducted by heating 175 g (0.623 mol) Empol 1008 and 70.8 g (0.685 mol) DEH20 at 160°C for 24 h under N_2 in a round-bottom flask. The product was dissolved in 250 g chloroform and excess DETA was removed by washing with a solvent blend of 300 g water and 120 g methanol. Chloroform was removed using a rotary evaporator and then followed by vacuum stripping for 24 h at 40°C. Added to a round-bottom flask was 200 g (0.547 mol estimated maximum available acid groups) of the amido-amine oligomer product and excess urea of 36.46 g (0.602 mol). The mixture was heated at 135°C for 1.5 h under N_2 flow before increasing the temperature by 5°C/h to 160°C. The ureido-amide elastomer was removed and cooled, then ground with a mortar and pestle into fine granules and washed with water for 72 h at 50°C and dried by vacuum stripping.

The ureido-amide elastomer was solubilized in a 50 : 50 mix of methanol and chloroform before a DGEBA epoxy resin, (D.E.R. 331 (Dow)) was added to the solvated mix at a calculated ratio of 10, 25, 50, and 100 mol % to overall amides in the elastomer. A 100 mol % addition is the calculated equivalent of a 1 : 1 ratio of epoxide to available amide groups from the ureido-amide elastomer based upon an estimated molecular weight of 5000 g/mol. The subsequent formulations utilized the same methodology such that the epoxide to amide ratios are estimated to be 0.5 : 1, 0.25 : 1, and 0.1 : 1 for the 50, 25, and 10 mol % epoxide formulations, respectively. About two-thirds of the solvent volume was removed by a rotary evaporator at 45°C and the remaining mix was vacuum stripped at −100 kPa and 100°C for 3 h. Attenuated total reflectance Fourier transform

Table I. Thermal and Fracture Properties of Epoxy-Ureido-Amide Polymer Blend

Mol epoxy (%)	0	10	25	50	100
$T_{g\ mDSC}$ (°C)	18	22	27	31	36
$T_{g\ DMTA—extrapolated\ onset}$ (°C)	8	18	28	40	47
T_{heal} (°C)	35	42	51	62	80
G_{IC} virgin (J/m2)	13 ± 2	21 ± 9	24 ± 8	72 ± 6	109 ± 4
G_{IC} healed (J/m2)	16 ± 1	45 ± 7	42 ± 9	40 ± 10	35 ± 7
G_{IC} recovery (%)	128	212	173	62	40

infrared (ATR-FTIR) spectroscopy was used to ensure that the solvent was removed without excessive crosslinking reactions taking place between the amine and epoxy prior to cure. The uncured blend was transparent at temperatures above 100°C suggesting good miscibility and then compression molded at 150°C for 6 h at 250 kPa to produce the final product which was again transparent. All cured blends were stored in a dry container with desiccant until required.

Characterization

DMTA spectra were obtained on a Pyris Diamond DMA (Perkin Elmer Instruments) in the dual cantilever mode at 1 Hz. Samples molded with dimensions of 20 × 10 × 3 mm^3 were heated at a rate of 2°C/min under nitrogen atmosphere from −50°C to 90°C. At all times, when discussing DMTA results, the glass transition temperature (T_g) was measured from the extrapolated onset of the decrease in the storage modulus. This was because for low epoxy content the peak in the tan δ spectra was often difficult to determine with confidence. Thermo-reversibility was investigated using DMTA on selected samples by performing a temperature ramp as described above followed by a subsequent cool down at the same rate and deformation frequency to −20°C. As a point of comparison the glass transition temperature was also determined using DSC using a mDSC model DSC2920 (TA Instruments) at 3°C/min modulated at (±1)°C under nitrogen gas flow for T_g analysis. ATR-FTIR spectroscopy was conducted on crushed samples using a Bruker Equinox 55 FTIR/NIR spectrometer. Samples were measured between 4000 and 600 cm^{-1} at a resolution of 4 cm^{-1} with an average of 64 scans. The microstructure of the virgin and healed samples were characterized by immediately coating with gold prior after fracture, on a Hitachi S5000 in-lens, cold field emissive high resolution microscope, at a 5kV accelerating voltage. Healing was characterized using SENB testing. Samples of dimensions 50 × 10 × 5 mm^3 with a 2.5 mm in-molded notch were fabricated, and prior to testing a 2 mm pre-crack was inserted into the notch using a sharp razor blade via careful tapping with a hammer. Samples were tested at 23°C using a 1 kN load cell in an Universal Testing Machine (Instron model 5569) according to ASTM D5045-99 until loss of load was detected. The fractured samples were placed in a clamping rig and subjected to heating in an oven for 2 h at temperatures correlating with an arbitrary DMTA change in modulus to 20 MPa for each formulation before SENB testing was repeated. This was done so that regardless of the extent of covalent or non-covalent bonding present, the softening of the polymer was the same. The healing temperatures used for each formulation are shown in Table I.

RESULTS AND DISCUSSION

Synthesis of Covalent and Physically Crosslinked Polymer Network

Prior to investigating the healing mechanism, it was necessary to characterize the structure of the polymer networks produced to ensure they contained both covalent and non-covalent bonding, rather than the epoxy being simply blended into the thermoplastic. As a preliminary guide to the formation of covalent crosslinking, the DSC residual exotherms before and after cure of each blend were determined. Though not shown here, they revealed negligible exotherms after cure, (compared with those prior to cure) indicating that cure reaction was complete, as much as can be asserted from the DSC technique. ATR-FTIR studies have also been used to explore the reaction between the epoxy and the ureido-amide thermoplastic. The thermoplastic is a complex mixture of fatty acids with various functional groups from amide, amine, and acid, and while it is difficult to be precise, ATR-FTIR studies do reveal formation of a polymer network through covalent reaction between the epoxy resin and thermoplastic. Figure 2(a) shows the overall changes of the spectra for different epoxy concentrations while Figure 2(b–e) give expanded views of specific functional groups. The most striking evidence for covalent bonding within the network is shown in Figure 2(b) which reveals the presence of a new peak at 1747 cm^{-1} which increases with increasing epoxy content. This peak directly relates to reaction between the epoxy and thermoplastic and may be attributed to an ester carbonyl peak which arises from well know epoxy acid reactions as shown in Figure 3(a). Also possible is a cyclization mechanism[20] as shown in Figure 3(b) representing an exchange of the nitrogen on the urea group with the oxygen from the hydroxyl group, reported to occur readily at moderately high temperatures. These changes confirm that reaction between the epoxy and urea groups was dependent upon the concentration of the epoxy resin after the initial epoxy ring-opening to form urea and a secondary alcohol. Figure 2(c,d) most likely reflects OH and C—O production respectively, as a consequence of the reaction with epoxy with an epoxy resin. Formation of alcohol groups is typical of the ring opening reaction of an epoxide group although homopolymerization or etherification could also explain these results.[21] Furthermore, Figure 2(e) complements the DSC studies to confirm that while epoxide conversion is difficult to

Applied Polymer SCIENCE

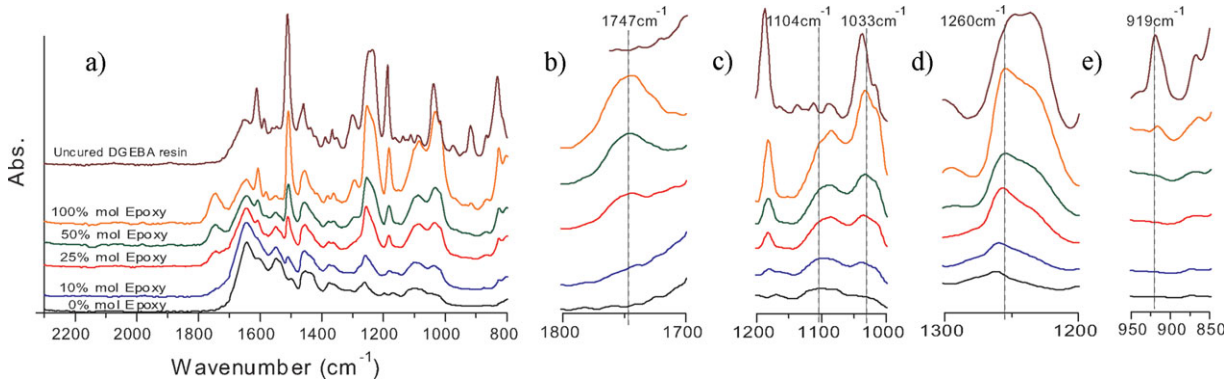

Figure 2. (a) Overview of the FTIR spectra for the cured ureido-amide epoxy blends at a varying epoxy levels. Expanded view of the (b) carbonyl region between 1700 and 1800 cm^{-1}, (c) hydroxyl region between 1000 and 1200 cm^{-1}, (d) C—O region 1200 and 1300 cm^{-1} and epoxide region between 850 and 950 cm^{-1}. [Color figure can be viewed in the online issue, which is available at wileyonlinelibrary.com.]

quantify, the relevant epoxide peak at 919 cm^{-1} for the cured blends is very small, indicative of high levels of conversion.

In addition to this, the polymer networks were all transparent regardless of the level of epoxy addition indicative of a homogenous microstructure and the lack of any phase separation. Further evidence of the formation of crosslinked network structures is provided by modulated DSC and DMTA results (Table I) which show consistent increases in the value of a single T_g with increasing epoxy content. The trends obtained from DSC and DMTA were also in agreement while the differences are due to the mode of measurement from mechanical to heat output changes. The raw DMTA spectra, as shown in Figure 4(a,b) for the elastic moduli and tan δ spectra, respectively, clearly illustrate the transformation from thermoplastic to thermosetting type behavior with increasing epoxy. The T_g (whether measured via the extrapolated onset of the loss of storage modulus or the tan delta maximum) clearly increases with increasing epoxy content. Below T_g, the storage modulus increases with increasing epoxy content, until the network becomes glassy in nature (from 25 mol % epoxy onwards), and then there is little difference between the subsequent samples. Above T_g, the storage modulus of the ureido-amide elastomer begins to display limited rubbery behavior, having a minimum storage modulus of about 10^5 Pa. At the same time, the tan δ spectra began to produce a peak displaying a clear maximum value. Overall, characterization of the modified ureido-amide elastomer using chemical and thermal analysis techniques has demonstrated formation of a hybrid network consisting of covalent and non-covalent bonding for a variety of epoxy concentrations. An idealized representation of the polymer network is shown in Figure 5 drawn from the above conclusions, illustrating the presence of both reversible (secondary) and non-reversible (primary covalent) bonds. Also shown in Figure 5 are the specific chemical segments involved in the reversible crosslinking reactions, showing that the hydrogen bonding between the carbonyl and nitrogen species are the basis for the reversible behavior.

Characterization of Thermo-Reversible Healing

A single thermal heating and cooling cycle was applied to the unmodified and epoxy modified (50% mol) ureido-amide elastomer using DMTA and the results are shown in Figure 6(a,b) respectively. The purpose of this experiment was to probe network mobility both within the glass state and above T_g, and compare it to the thermo-reversible behavior (as measured by storage modulus) exhibited by the networks with and without covalent crosslinks. In this way, the effect of incorporating covalent, non-reversible bonds could be compared with networks containing only thermo-reversible bonds. As can be seen, contrary to the unmodified elastomer, which displayed recovery of the storage modulus even higher than the initial modulus after cooling, the storage modulus of the epoxy modified ureido-amide elastomer was not fully restored. This observation was true even when varying the maximum cycling temperatures as shown

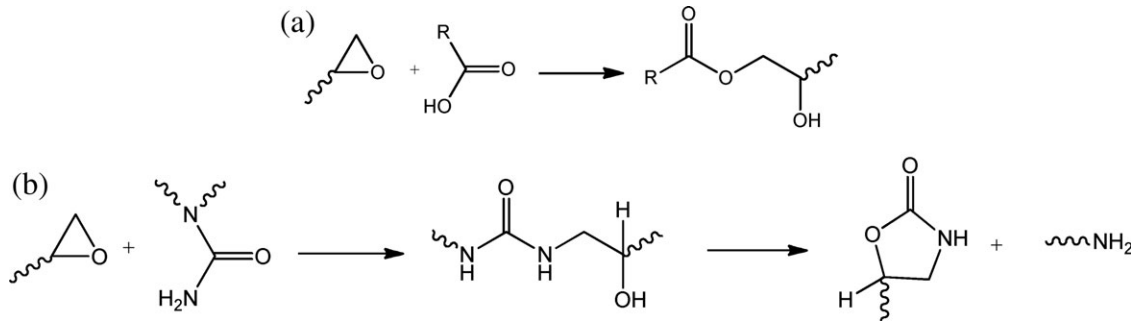

Figure 3. Potential mechanism to produce the ester linkages suggested by the FTIR spectra for (a) which present the epoxy acid reaction while (b) proposes a ring opening mechanism between epoxy and amide species leading to a cyclized ester functionality.

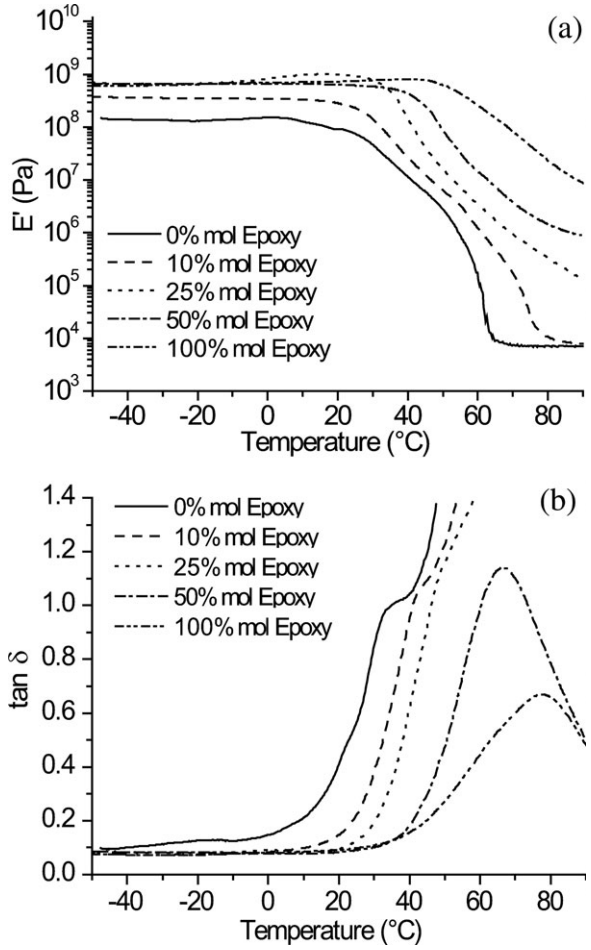

Figure 4. DMTA analyses for the ureido-amide epoxy blends at a varying epoxy levels highlighting the transformation from thermoplastic to thermosetting behavior for the (a) storage modulus and (b) tan δ spectra.

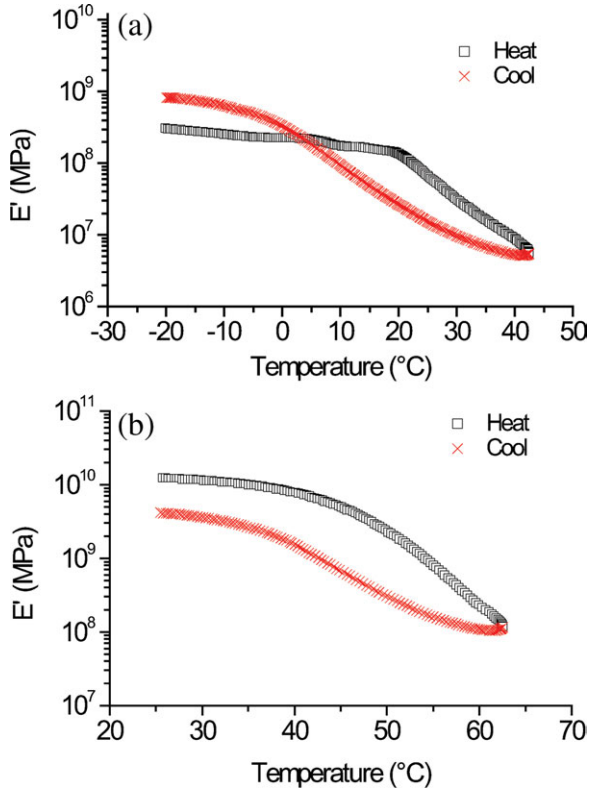

Figure 6. DMTA storage modulus characteristics upon heating and cooling of (a) an unmodified and (b) a 50% mol epoxy modified ureido-amide elastomer. [Color figure can be viewed in the online issue, which is available at wileyonlinelibrary.com.]

in Figure 7(a)which plots the extent of modulus recovery against the difference between the maximum cycling temperature and the glass transition temperature ($T_{max} - T_g$). Analysis of the rate of recovery, (i.e., comparison between the rate of storage modulus decrease against the rate of storage modulus increase) plotted against the $T_{max} - T_g$ [Figure 7(b)] also shows the inhibiting effect of the increased covalent crosslinking within the epoxy modified ureido-amide elastomer. It is interesting to note that increasing the maximum temperature increased the rate and extent of recovery regardless of whether

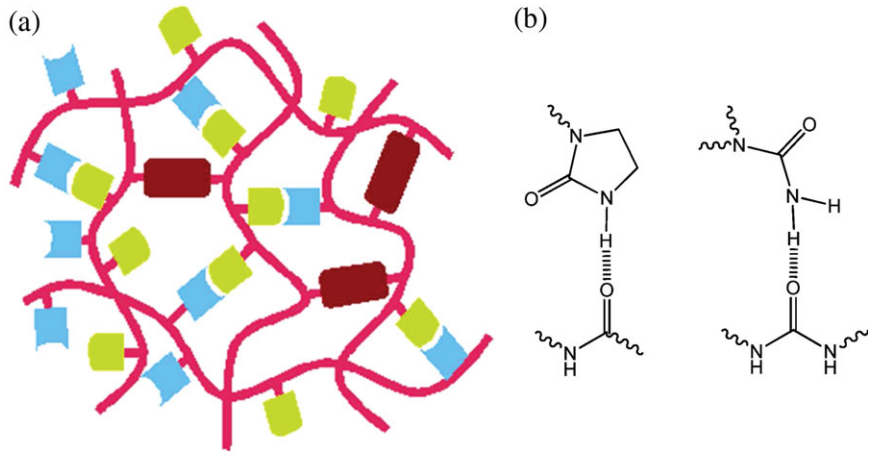

Figure 5. (a) Schematic representation of the crosslinked supramolecular polymer containing covalent (non-reversible-red blocks) and non-covalent (reversible-blue/green blocks) bonds. (b) Illustration of the likely reversible hydrogen bonding taking place between the amides, urea and imidazole, and functionality. [Color figure can be viewed in the online issue, which is available at wileyonlinelibrary.com.]

Applied Polymer SCIENCE

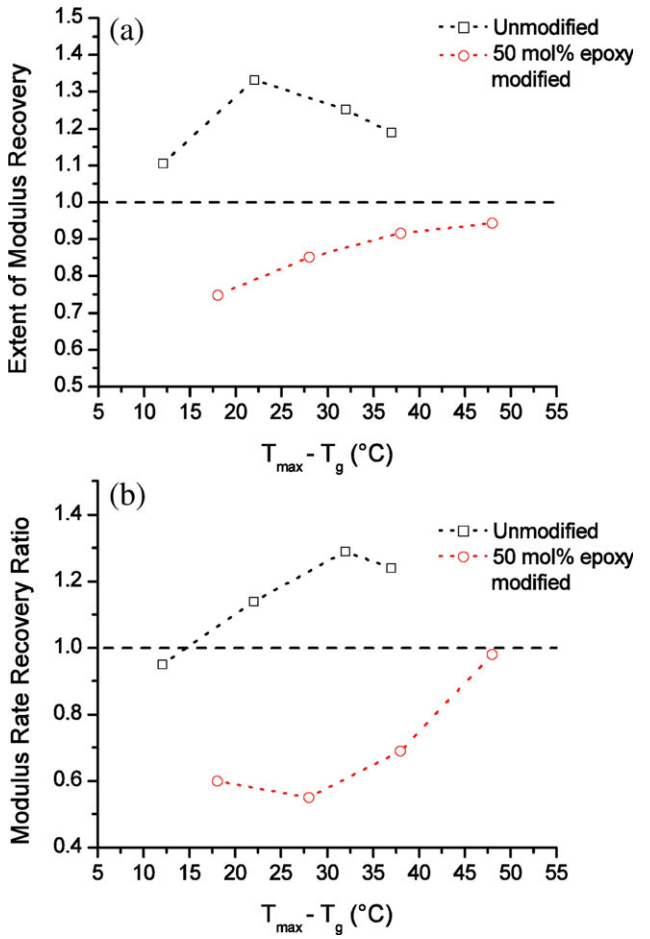

Figure 7. (a) Extent of modulus recovery and (b) modulus rate recovery ratio of the unmodified ureido-amide elastomer compared to an epoxy modified (50% mol) elastomer across various maximum cycle temperatures above T_g. [Color figure can be viewed in the online issue, which is available at wileyonlinelibrary.com.]

the ureido-amide elastomer was modified or not. It is suggested that higher molecular mobility within the non-covalent based polymer network facilitates optimum chain rearrangement and minimum energy configurations, promoting better chain packing, higher modulus, and higher rates of recovery as the temperature reduces below T_g. Another possible explanation for this improvement in the extent and rate of modulus recovery is that higher temperatures provide greater molecular mobility in the rubbery phase and more potential reaction between residual functional groups. As the temperature decreases from above the glass transition it is possible that this may produce moduli values greater than the initial modulus. Nonetheless, these findings show that even a highly modified ureido-amide polymer network containing covalent crosslinks can still display extensive thermo-reversible healing, despite the inhibiting effect of the non-reversible covalent crosslinks. Figure 7(a) illustrates this clearly because at a healing temperature about 16°C above T_g, for the 50 mol % epoxy sample, the modulus still recovers about 75% of its initial value, while at temperatures almost 50°C above the T_g, over 90% recovery is achieved for the same sample.

The recovery in modulus and the increased rate of recovery with temperature cycling clearly reflects the level of molecular mobility and thermo-reversibility in the absence of any actual catastrophic damage to the ureido-amide polymer network. More specifically this is expected to arise from less chain entanglements between the different types of crosslinking. To characterize healing after a damage event, and to gain an insight into molecular mobility and thermo-reversibility across a fracture plane, SENB testing has been performed. Table I and Figure 8 show the critical strain energy release rate (G_{IC}) of the epoxy-ureido-amide blends before and after healing as a function of epoxy content at 23°C. The virgin unmodified ureido-amide elastomer displays poor fracture properties, well below that of conventional engineering thermoplastics, however as epoxy content increases, the G_{IC} increases with increasing covalent bonding, crosslink density, and approaching values expected of typical epoxy resins.[17] The G_{IC} values after healing as shown in Figure 8 are relatively constant as a function of epoxy content, decreasing very slightly with high concentrations of epoxy resin. To this extent, the healing efficiency as measured by the ratio of the healed and virgin G_{IC} values is controlled by the G_{IC} of the virgin polymer blend which gets tougher with increasing epoxy content. Thus at lower levels of epoxy addition, the healing efficiencies are very high, exhibiting over 200% recovery. Excellent healing of this order may be a result from the absorption of moisture from the air and subsequent plasticization due to the hydroscopic nature of the material. The large G_{IC} recovery for the 10 mol % epoxy modified sample in particular is approximately twice the value of the healed unmodified sample is remarkable (i.e., 200% healing). At this concentration, the glass transition temperature is very close to room temperature, so care needs to be taken when interpreting G_{IC}. Despite this the results compare well with other formulations and are therefore considered to have value. Other possible reasons for this very high level of healing may relate to the formation of hydroxyl groups during epoxy cure which generate more hydrogen bonding with carbonyl groups compared with NH groups. The

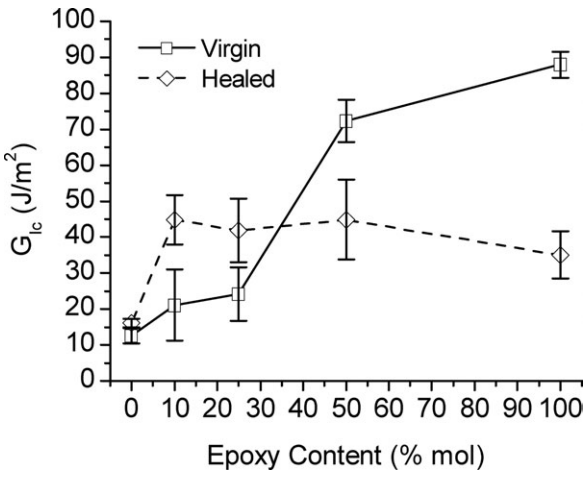

Figure 8. Strain energy release rate before and after healing as a function of epoxy mol%.

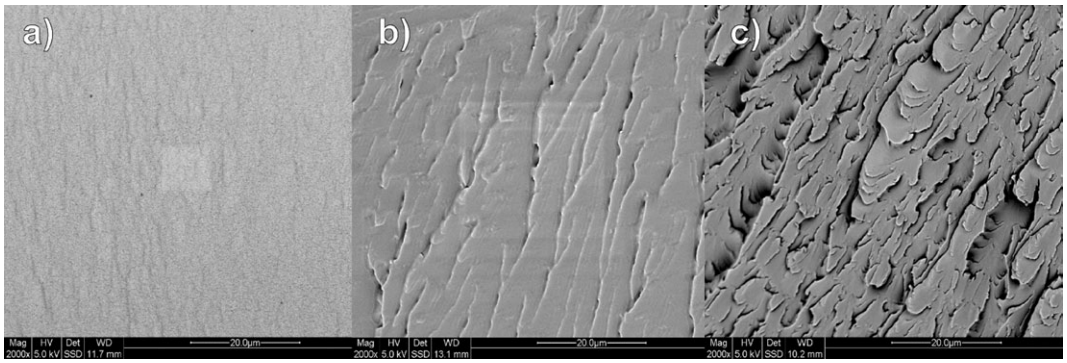

Figure 9. Back-scattered electron SEM image showing fracture surface of SENB samples of (a) a virgin unmodified ureido-amide elastomer, (b) a virgin blend containing 50% mol epoxy added, and (c) a healed blend containing 50% mol epoxy added.

residual functionality after cure may also improve healing through further covalent bonding providing another mechanism for higher recovery. It is also worth noting that at these lower concentrations of epoxy content, the system was able to be molded like a thermoplastic then set into place.

Clearly the balance between covalent and non-covalent bonding is what determines the level of healing. As covalent bonding increases and molecular mobility decreases the extent of healing decreases. However, it is important to note that even at epoxy concentrations which produced a polymer network with enhanced elastic properties, for example, at 50 mol % of epoxy, healing remains high, still exhibiting a recovery of over 60%. Despite this thermo-reversible behavior, it is also clear that the presence of epoxy resin does in fact inhibit molecular mobility complementing the findings from thermal analysis. The SEM fracture surfaces shown in Figure 9(c) is of a healed 50 mol % epoxy modified samples that has been manually cleaved after a single healing event. The fracture surface shown remains similar to that of the virgin 50 mol % epoxy modified material [Figure 9(b)] indicating a similar failure mechanism after healing even though the shear bands for the healed samples appear slightly more hackled. Figure 9(a) shows the smooth featureless surface evident for the pure ureido-amide elastomer.

CONCLUSION

An ureido-amide thermoplastic elastomer wholly reliant on supramolecular chemistries was tuned with various levels of covalent bonds by reacting with DGEBA. Evidence of a chemical reaction between the epoxy and the amide groups of the thermoplastic was provided by FTIR while DMTA results showed changes from a material characteristic of a thermoplastic to that more representative of a thermoset as the epoxy concentrations were increased. DMTA thermal cycling showed that the addition of epoxy reduced the extent and rate of thermo-reversible behavior to impact the recovery of the storage modulus. Similar behavior was observed for the recovery of the fracture properties, decreasing with increasing epoxy content. This system demonstrated improved virgin fracture properties and subsequent fracture toughness healing efficiencies from over 200% to 40% depending on the levels of epoxy used. The results also show that even when the T_g of the polymer network is above room temperature and there is significant covalent bonding, extensive molecular mobility continues to facilitate significant thermo-reversible healing.

ACKNOWLEDGMENTS

The authors thank Januar Gotama and Tri Nguyen for providing advice in the processing and manufacture of the polymer blend.

REFERENCES

1. Brunsveld, L.; Folmer, B. J. B.; Meijer, E. W.; Sijbesma, R. P. *Chem. Rev.* **2001**, *101*, 4071.
2. Cordier, P.; Tournilhac, F.; Soulie-Ziakovic, C.; Leibler, L. *Nature* **2008**, *451*, 977.
3. Montarnal, D.; Cordier, P.; Soulie-Ziakovic, C.; Tournilhac, F.; Leibler, L. *J. Polym. Sci. Part A: Polym. Chem.* **2008**, *46*, 7925.
4. White, S. R.; Sottos, N. R.; Geubelle, P. H.; Moore, J. S.; Kessler, M. R.; Sriram, S. R.; Brown, E. N.; Viswanathan, S. *Nature* **2001**, *409*, 794.
5. Trask, R. S.; Bond, I. P. *Smart Mater. Struct.* **2006**, *15*, 704.
6. Chen, X.; Wudl, F.; Mal, A. K.; Shen, H.; Nutt, S. R. *Macromolecules* **2003**, *36*, 1802.
7. Hayes, S. A.; Zhang, W.; Branthwaite, M.; Jones, F. R. *J. R. Soc. Interface* **2007**, *4*, 381.
8. Meure, S.; Wu, D. Y.; Furman, S. *Acta Mater.* **2009**, *57*, 4312.
9. Varley, R.; Van der Zwaag, S. *Polym. Int.* **2010**, *59*, 1031.
10. Chino, K.; Ashiura, M. *Macromolecules* **2001**, *34*, 9201.
11. Peng, C. C.; Abetz, V. *Macromolecules* **2005**, *38*, 5575.
12. Stadler, R.; de Lucca Freitas, L. *Colloid Polym. Sci.* **1986**, *264*, 773.
13. Lange, R. F. M.; Van Gurp, M.; Meijer, E. W. *J. Polym. Sci. Part A: Polym. Chem.* **1999**, *37*, 3657.

14. Yamauchi, K.; Kanomata, A.; Inoue, T.; Long, T. E. *Macromolecules* **2004**, *37*, 3519.
15. Dimopoulos, A.; Wietor, J.-L.; Wubbenhorst, M.; Napolitano, S.; van Benthem, R. A. T. M.; de With, G.; Sijbesma, R. P. *Macromolecules* **2010**, *43*, 8664.
16. Wietor, J. L.; Dimopoulos, A.; Govaert, L. E.; van Benthem, R.; de With, G.; Sijbesma, R. P. *Macromolecules* **2009**, *42*, 6640.
17. Wietor, J.-L.; Sijbesma, R. P. *Angew. Chem. Int. Ed.* **2008**, *47*, 8161.
18. Montarnal, D.; Tournilhac, F.; Hidalgo, M.; Leibler, L. *J. Polym. Sci. Part A: Polym. Chem.* **2010**, *48*, 1133.
19. Tournilhac, F.; Cordier, P.; Montarnal, D.; Soulie-Ziakovic, C.; Leibler, L. *Macromol. Symp.* **2010**, *291*, 84.
20. Bosc, J.; Jarry, C.; Léger, J.; Négrier, P.; Haget, Y. *J. Chim. Phys. Phys. Chim. Biol.* **1995**, *92*, 1066.
21. Pascault, J.-P.; Sautereau, H.; Verdu, J.; Williams, R. J. J. Thermosetting Polymers; Marcel Dekker, Inc.: New York, **2002**.